

# Photometry on Eclipsing Polar MASTER OT0614-27

Edrei Chua, Natalia Drozdoff, Krystyna Miles, and Jack Neustadt

*Department of Physics & Astronomy, Dartmouth College, Wilder Laboratory, Hanover, NH, USA*

## ABSTRACT

MASTER OT J061451.70-272535.5 was observed photometrically at the South African Astronomical Observatory (SAAO) at Sutherland using the 1.9 m and 1.0 m telescopes (Buckley et al. 2015). Preliminary investigation of the light curve obtained on 24 February 2014 revealed a distinct double eclipse. Subsequent spectroscopic observations by the South African Large Telescope (SALT) suggest that MASTER OT0614-27 is a magnetic cataclysmic variable. With photometric data from both the 1.9 m and 1.0 m telescopes, there is strong evidence that MASTER OT0614-27 is an eclipsing polar. This paper analyses the photometric data obtained during the end of February and beginning of March of 2015 to find a period. The period is calculated to be  $0.0865884 \pm 0.0000107$  days.

*Subject headings:* MASTER OT0614-27, Eclipsing Polar, Photometry, SAAO

## 1. Introduction

A new cataclysmic variable (CV) star catalogued as MASTER OT J061451.70-272535.5 (hereafter MASTER OT0614-27) was discovered by MASTER-SAAO on 2015-02-19.96990 UT in Sutherland, South Africa. It is located at RA  $06^{\text{h}} 14^{\text{m}} 51.70^{\text{s}}$  and Dec  $27^{\circ} 25' 35.5''$  with an unfiltered magnitude of 18.3 mag with a limit of 19.4 mag. A total of five images were collected in the MASTER-SAAO database, and a reference image from 2015-02-06.92896 UT was used with a 19.4 unfiltered magnitude limit (Shumkov et al. 2015).

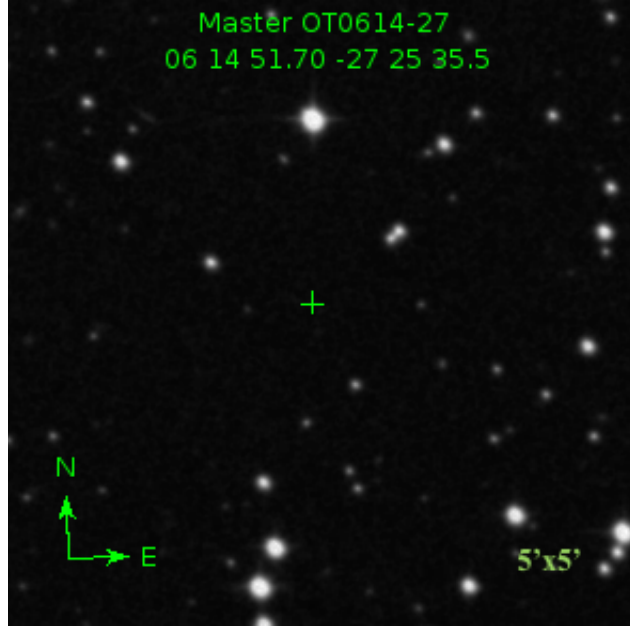


Fig. 1.— This is a finding chart for the MASTER Source. It was made using the Sloan Digital Sky Survey images.

The goal of the Mobile Astronomical System of Telescope Robots (MASTER) survey was to generate a unique fast sky survey that included the entire sky observed over a single night down to a magnitude of 19-20. Launched in 2002, the project made it possible to continue the quest to understand dark energy via the discovery and photometry of supernovae, microlensing effects, exoplanets, and minor bodies in the solar system (Lipunov et al. 2010).

Cataclysmic Variable stars (CVs), such as MASTER OT0614-27, are binary stars that are composed of a white dwarf primary star and a mass transferring secondary star. A white dwarf is the endpoint of stellar evolution for a low-mass star. White dwarfs are of interest because they represent a history of star formation and their luminosities serve as a lower limit on the age of the Galactic disk. The local population is comprised of several classifications of white dwarfs: DA stars are H-rich; DB are He-rich; DC stars have continuous spectra; DQ stars have carbon features; DZ have metal lines only; WD+MS stars are white dwarf and main sequence binary systems; and WD+WD stars are double degenerate systems (Holberg et al. 2002).

MASTER OT0614-27 is specifically an AM Hercules star, a type of CV that is a close binary star in which matter transfers via Roche lobe overflow from a dwarf secondary star onto a magnetic white dwarf primary star. The white dwarf's magnetic field strength (**B** on the order of 100 megagauss) is so strong that it synchronizes the spin period of the

white dwarf to match the binary orbital period. The accretion flow then attaches on to the magnetic field lines of the white dwarf. This causes the accretion flow to be directed out of the orbital plane and travel along the magnetic field lines in order to form a shock above the white dwarf. The post-shock region has a temperature hot enough for hard X-rays to be emitted. A polarized cyclotron emission in the region is caused by electrons circulating around the magnetic field lines (Ramsay et al. 1996).

## 2. Method

The data on MASTER OT0614-27 in this paper was collected using three of the telescopes at SAAO at Sutherland in South Africa. Those telescopes included a 1.9 m telescope, a 1.0 m telescope and SALT. Both the 1.9 m and the 1.0 m are optical telescopes that were used along with CCD SHOC cameras to create data cubes (Coppejans et al. 2013). A series of integrations were taken as data cubes, the details of which can be seen in the observing log in Table 1. These observations were spread out over a range of evenings from 24 February 2015 to 1 March 2015.

Image	Date obs.	Filter	Num. of Exp.	Exp. Time (s)	Binning	Airmass	Start Time (JD-2457000)	End Time (JD- 2457000)
74-10	2/24/15	Open	825	15	8x8	1.006	78.26262	78.40382
74-1	2/25/15	Open	1251	10	8x8	1.005	79.26498	79.40951
74-8	2/26/15	Open	1391	10	10x10	1.005	80.28042	80.44117
74-1	2/27/15	Open	1200	10	8x8	1.004	81.26182	81.40068
74-9	2/28/15	B	900	15	8x8	1.013	82.28984	82.44424
40-14	2/28/15	R	320	45	2x2	1.007	82.27978	82.44490
74-1	3/1/15	Open	560	10	8x8	1.092	83.27181	83.33621

Table 1: This table lists the observing log for the data used for MASTER OT0614-27.

On 28 February 2015, the 1.0 m telescope and SALT both examined this source in addition to the 1.9 m. SALT collected spectroscopic data while the 1.0 m collected data using the R filter and the 1.9 m collected data using the B filter.

These observations were then reduced using Professor John Thorstensen’s pipeline. This pipeline allows the user to assign headers to each of the data cubes, subtract out the biases, divide by the flats, and then perform differential photometry on the target star as well as several reference stars for each frame of the data cube. Those stars are all visible and annotated in Figure 2.



Fig. 2.— This is a sample of one of the frames from one of the data cubes with the stars used for analysis identified in green.

There are a couple notes of interest regarding this data reduction. First, while most were divided by the appropriate flat, it was impossible to divide the B filter data by a B filter flat because the B filter was not received in time. Instead, an open filter flat was used. While this is imperfect, it is sufficient for the data at hand. Next, a few of the observations were GPS triggered while most of them were not. This led to some slightly different work within the pipeline but should not have had an effect on the final results.

### 3. Analysis

#### 3.1. Open Filter Data

MASTER OT0614-27 was first observed eclipsing on February 24, 2015. This first observation serves as a zero point for cycle numbers when calculating the period, and its light curve is shown below in Figure 3. Unfortunately, due to clouds, poor seeing, and high humidity conditions, it is difficult to see some details in the star's light curve especially at the end. However, a couple of interesting features are apparent. First, the egress from the eclipse is very sharp and clearly visible even with the poor conditions. Also visible is a small dip prior to the full eclipse.

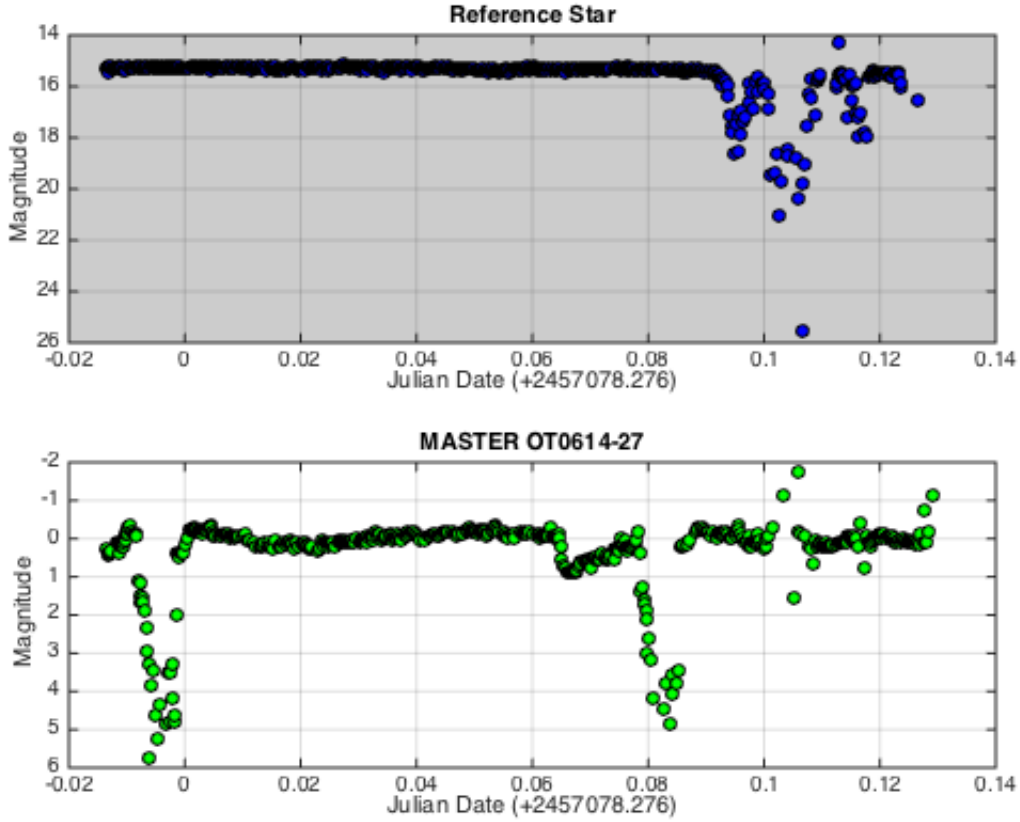


Fig. 3.— This is a light curve for the MASTER OT0614-27 on the 24th of February 2015. The MASTER source is the green data and the comparison stars are the blue data. This was the first observed eclipse of the star and serves as the zero point for the cycle numbers. The x-axis is the time as a Julian Date from the time of the first eclipse. The y-axis is a magnitude value.

The initial dip prior to the eclipse is repeated prior to each eclipse, as is visible in Figure 4, and is not simply a product of poor observing conditions. It is not yet clear what this initial dip is. It could be due to the obscuring of an accretion stream prior to the eclipse of the star. The issue with this interpretation is that it may not fully account for the increase in the light curve prior to the large eclipse. If the initial dip were purely due the obscuring of the accretion stream prior to the obscuring of the star, the expected curve would not increase prior to the full eclipse as was noted by Professor John Thorstensen. Therefore, it is possible that something else is going on in the system.

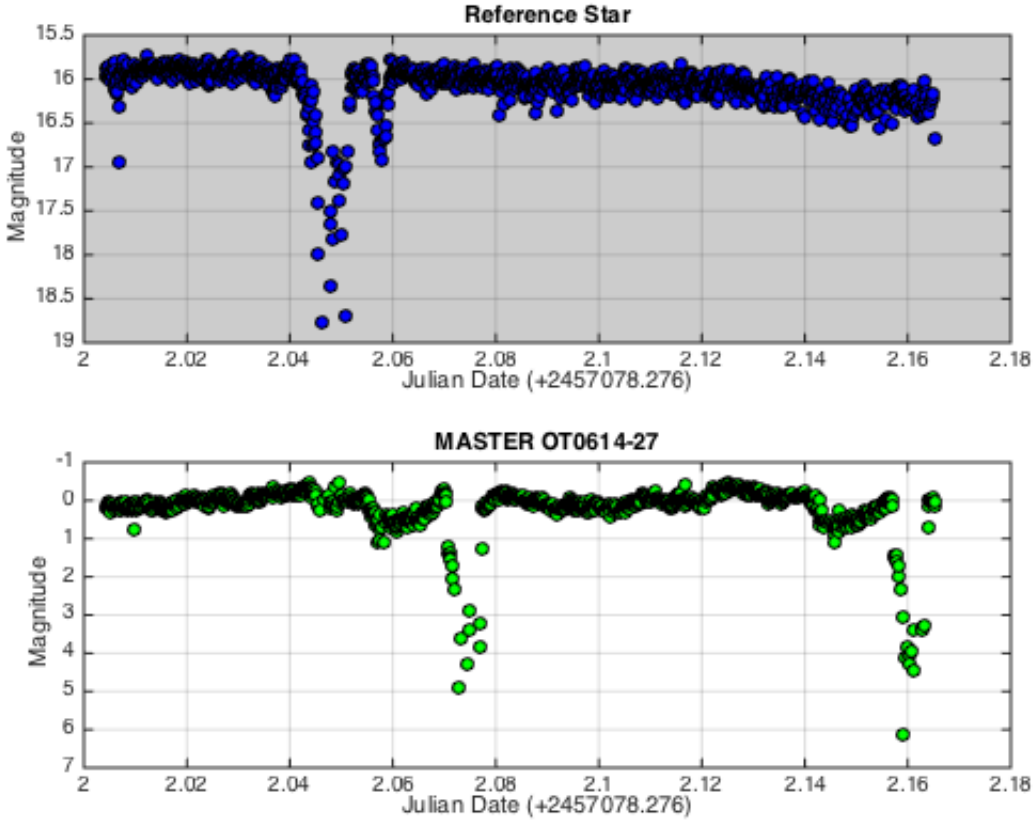


Fig. 4.— This is a light curve for the MASTER OT0614-27 on the 26th of February 2015. The egress on the first eclipse and initial dip is very clear here.

An approximate period can be gained by looking at the time between the egress of the two eclipses in Figure 3. This period is about 0.0868 days, or a little over 2 hours. This approximate period can then be refined further by looking at the period values calculated by measuring the period using different repeating points in the same light curve and looking at other pairs of consecutive eclipses like the one in Figure 4 and the pairs shown in the Appendix. The data measured from these curves is shown in Table 2.

	20150224	20150225	20150226	20150227	20150301
Small Dip Ingress	–	79.29127	80.32953	81.2829	83.27691
Small Dip Min.	–	79.29498	80.33393	81.28638	83.27923
Small Dip Egress	78.26592	79.30320	80.34493	81.29842	83.29081
Large Dip Min.	78.27200	79.30957	80.35141	81.30340	83.29648
Large Dip Egress	78.27634	79.31432	80.35454	81.30699	83.29810
Small Dip Ingress	78.33956	79.37628	80.41685	81.37092	–
Small Dip Min.	78.34217	79.38056	80.42055	81.37277	–
Small Dip Egress	78.35276	79.39237	80.43121	81.38470	–
Large Dip Min.	78.35971	79.39596	80.43665	81.38945	–
Large Dip Egress	78.36318	74.40094	80.44013	81.39339	–

Table 2: The first column of this table lists the event that occurred. The second column lists the time at which that occurred during observing on the night listed at the head of each column. The times are given as a Julian Date minus 2457000.

An approximate period can be gained by taking the difference between any pair of matching values in the two different sections of the same column. For example the difference between the egress of the first large dip in the first column and the second large dip in the first column is 0.08684, which is a basic approximation of those periods. These are pairs of consecutive repeating events in the system.

The approximate values for the period can then be averaged to find a good approximation for the period, which can be used to find cycle numbers. Several of the periods and an average period are shown below in Table 3. It is not necessary to repeat this step for every single possible measurement point on every eclipse because an approximation is all that is needed. It is necessary for the approximate period to be sufficiently accurate for the cycle counts found later to be within a couple tenths of their integer. In this case, it was only necessary to use the eclipses from the 27th, 26th, and 24th to get an approximate period that was good enough to get accurate cycle numbers.

	20150227	20150226	20150224
Large Eclipse Min.	0.08605	0.08524	0.08771
Small Eclipse Min.	0.08639	0.08662	
Large Eclipse Egress	0.08640	0.08559	0.08684
Small Eclipse Egress	0.08628	0.08628	0.08684
Small Eclipse Ingress	0.08802	0.08732	
Average	0.08658		

Table 3: This table includes all the calculated values for period measuring between different points for each frame with two consecutive eclipses.

The resulting approximation of the period is 0.0866 days which is equal to 2.078 hours. This value for period can then be used to assign cycle numbers to each eclipse using

$$P = \frac{t_N - t_0}{N}. \quad (1)$$

The cycle numbers listed in Table 4 can be found by subtracting the time of the first observation of the large eclipse egress in the data cube from 20150224 from the large eclipse egress of the eclipse under examination and dividing by the approximate period given in Table 3. The calculation yields values that are within a few hundredths of, but not exactly, whole numbers. Since the cycle number must be a whole number the value is then rounded to the nearest whole number.

Cycle Number	JD of Large Eclipse Egress -2457000
0	78.27634
1	78.36318
12	79.31432
13	79.40094
24	80.35454
25	80.44013
35	81.30699
36	81.39339
58	83.29810

Table 4: This table lists the cycle number and Julian Date of each eclipse's ingress minus 2457000.

These values can then be plotted. When a linear regression is fit to this plot, the resulting equation is the ephemeris for the system. This is shown in Figure 5.

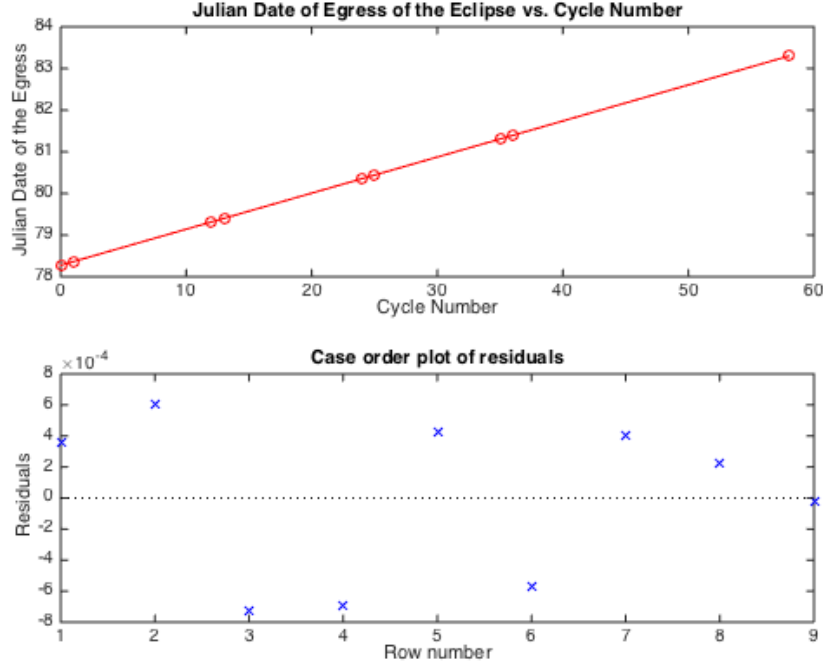


Fig. 5.— The first plot is a plot of the Julian Date of the Egress for each eclipse vs. the Cycle Number for the eclipse. The second plot is a graph of the residuals for the linear regression.

Based on this linear regression, the ephemeris for the system is

$$\text{Time of Eth Eclipse Egress} = 78.27599 + 0.0865884E. \quad (2)$$

The period of the system is therefore 0.0865884 with a standard error of  $\pm 0.0000107$  days. This is equivalent to 2.07812 with a standard error  $\pm 0.000257$  hours. The R-squared value for this regression is approximately 1.

### 3.2. R and B Filter Data

MASTER OT0614-27 was observed through the red filter (R) and the blue filter (B) at approximately the same time on 28 February 2015 in order to investigate potential changes

in color during the course of the eclipse.

The target star system was observed using separate telescopes concurrently - R filter with the 1.0 m telescope and B filter with the 1.9 m telescope. The light curves obtained using the R and B filter are overlaid with each other in a single graph in Figure 6. It is evident from visual inspection of Figure 6 that the red magnitude and blue magnitude of MASTER OT0614-27 exhibit similar trends, which seems to suggest that the system did not experience a change in color magnitude over the course of the eclipse.

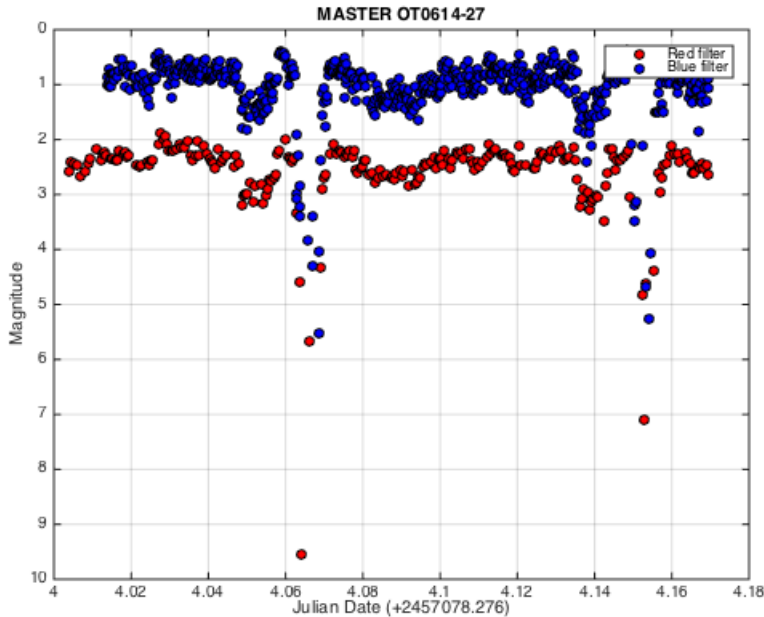


Fig. 6.— This is the overlayed B and R light curves for MASTER OT0614-27 obtained on 28 February 2015

The next step is to obtain a B-R light curve to confirm the hypothesis formulated from visual inspection of Figure 6. It should be noted that different exposure times were used for observations through the R filter and B filter; the exposure time for the 1.0 m telescope observing in the R bandwidth was set at 45.0 seconds while the exposure time for the 1.9 m telescope observing in the B bandwidth was set at 15.0 seconds. Therefore, there are 320 images obtained with the R filter and 900 images obtained with the B filter over approximately the same time period. As a result, it is necessary to match the time of the light curves obtained with the R filter and the B filter as closely as possible so that the comparison made by the B-R light curve makes physical sense. This can be accomplished using several methods, two of which were attempted here- the matching method and the

averaging method.

The first approach, or the matching method, compares the time in Julian date of the B photometric data with the R photometric data and plots the data point for B-R on a graph if and only if the time matches to three decimal places. This would ensure that fluctuation in B-R is accurate over a time interval of  $0.0010 \pm 0.0005$  days, which translates to  $0.024 \pm 0.012$  hours. The B-R light curve obtained using the matching method is presented in Figure 7. The temporal data for both light curves are obtained using a GPS trigger, which yield a precision of 0.0000001 day. Theoretically, the matching can be increased to a precision up to 7 decimal places (in Julian date), but the tradeoff for increasing the precision is having fewer data points to plot.

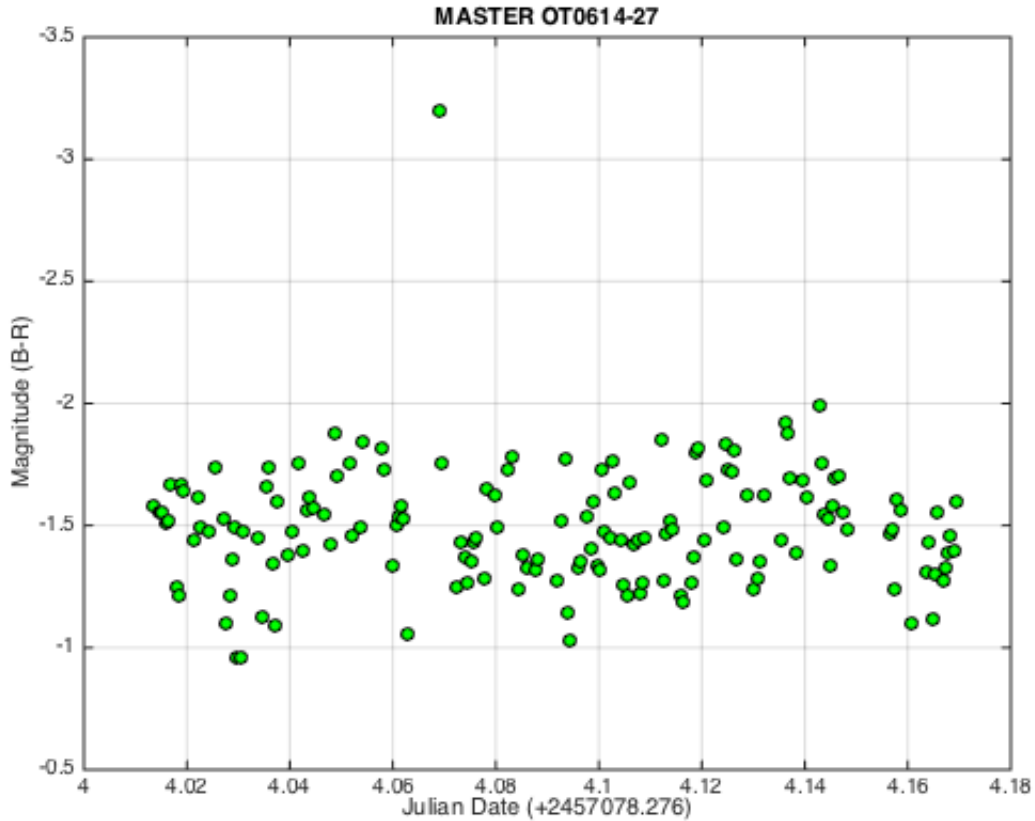


Fig. 7.— This is a the B-R light curve for MASTER OT0614-27 obtained on 28 February 2015 using the matching method

The second approach, or the averaging method, averages three of the 15.0 seconds

exposure obtained using the B filter. This would ensure that the time interval for comparison is fixed at 45 seconds, since the averaging for the B filter is over a duration of  $3 \times 15.0 = 45.0$  seconds and the exposure time for the R filter is 45.0 seconds. The first 20 exposures for the R photometric data were not used because observation with the R filter commences slightly before observation with the B filter. This entire process ensures that there are 300, 45 second exposures with the R filter and 900, 15 second exposures with the B filter, which makes it convenient since we can compare photometric data at a time interval of 45 seconds over a course of  $300 = 900 \times 15 = 13500$  s = 3.75 h. Figure 8 shows the B-R light curve obtained using the averaging method.

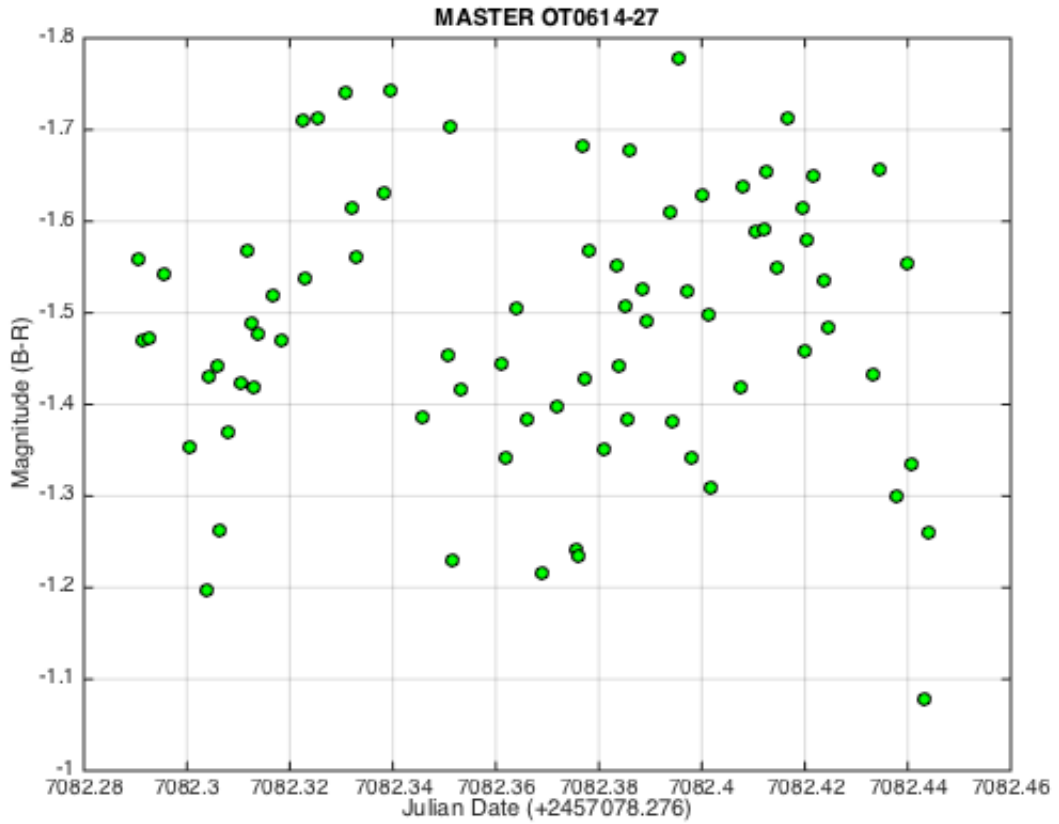


Fig. 8.— This is a the B-R light curve for MASTER OT0614-27 obtained on 28 February 2015 using the averaging method

In both cases, it can be noted that the data points are scattered randomly about a mean value of -1.5 mag (B-R). This leads to the conclusion that that there is no observable trend in the B-R light curve for MASTER OT0614-27.

#### 4. Results

There are a couple important results about the polar MASTER OT0614-27 which come out of this analysis. The first is that the period of the of the eclipse is 0.0865884 with a standard error of  $\pm 0.0000107$  days or about  $2.07812 \pm 0.000257$  hours. This comes from the analysis of the time and cycles between nine eclipses.

The second major result concerning this source is that the color of the system remains constant throughout the eclipse. This comes from the B-R data discussed in the analysis section. Since the data is scattered, it is apparent that the eclipse does not result in a noticeable change in color.

#### 5. Discussion and Conclusion

The basic analysis done in this paper establishes guidelines for understanding the MASTER OT0614-27 source. The initial period calculations and information regarding the color data collected lay a ground work for future investigations. Those investigations have much to work with in this interesting system from finding the period with even greater precision than has been done in this paper to developing an understanding of the unusual qualities of the initial dip in the eclipse. That initial dip has the potential to be a very interesting source for future investigation. As noted earlier, in the beginning of the analysis section, there are some hypotheses regarding the physical interaction that it corresponds to but as of yet, its nature is not obvious. Hopefully, this issue will be addressed in future astronomical work on this object.

#### 6. Acknowledgements

The authors acknowledge the help provided throughout by Professor Thorstensen without whom this paper would not have been possible. They would also like to thank Hannes Breytenbach and Mokhine Motsoaledi for their work collecting the data from the 1.9 m and 1.0 m telescopes analyzed in this paper. They would also like to thank their TAs, Erek Alper and Mackenzie Jones.

#### REFERENCES

Buckley, A.H., Breytenbach, J., Kniazev, A. et al., 2015, ATel #7169.

Coppejans, R., Gulbis, A.S., Kotze, M.M. et al., 2013, PASP, 125, 976-988.

Holberg, J. B., Oswalt, T. D., & Sion, E. M. 2002, ApJ, 571, 512

Lipunov, V., Kornilov, V., Gorbovskoy, E., et al. 2010, Advances in Astronomy, 2010, 349171

Ramsay, G., Cropper, M., Wu, K., & Potter, S. 1996, MNRAS, 282, 726

Shumkov, V., Balanutsa, P., Gress, O., et al. 2015, The Astronomer’s Telegram, 7127, 1

## 7. Appendix

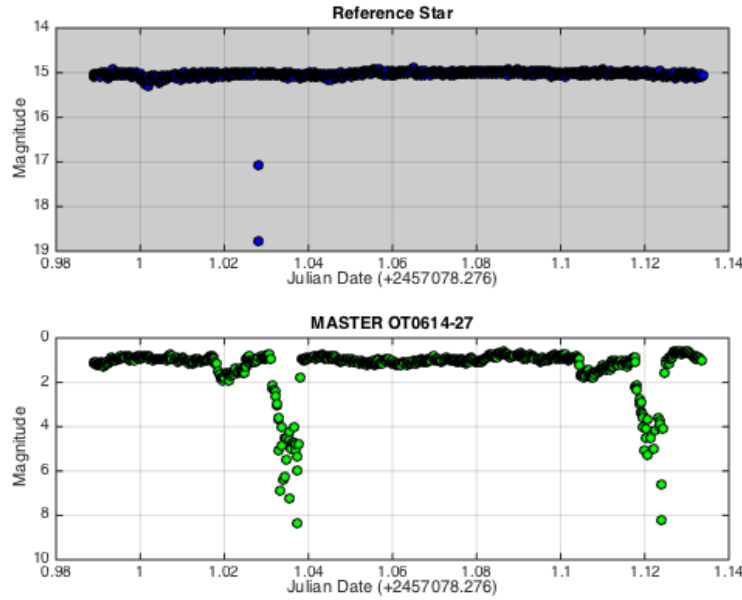


Fig. 9.— This is a light curve for the MASTER OT614-27 on the 25th of February 2015. It is obtained with the 1.9 m telescope using an open filter.

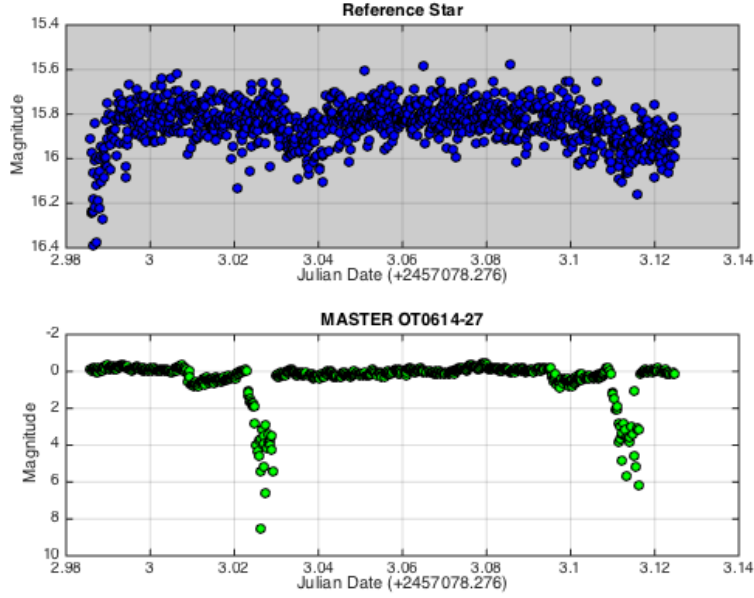


Fig. 10.— This is a light curve for the MASTER OT614-27 on the 27th of February 2015. It is obtained with the 1.9 m telescope using an open filter.

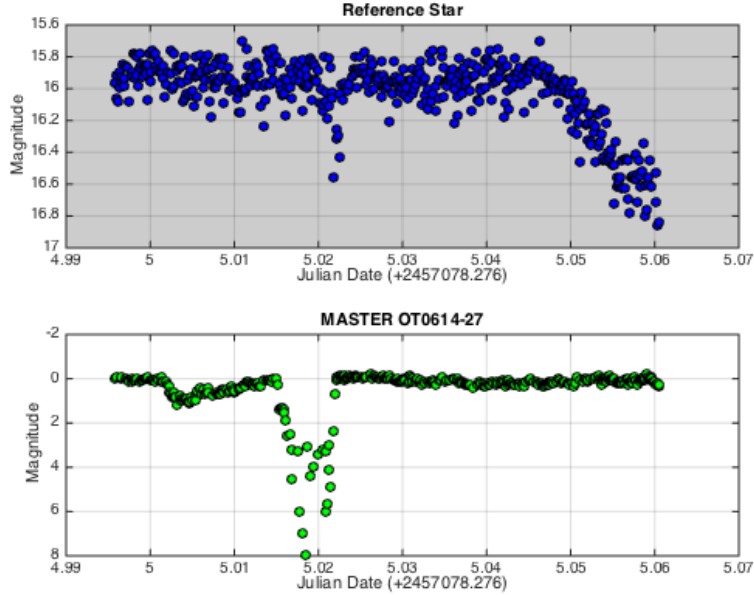


Fig. 11.— This is a light curve for the MASTER OT614-27 on the 1st of March 2015. It is obtained with the 1.9 m telescope using an open filter.

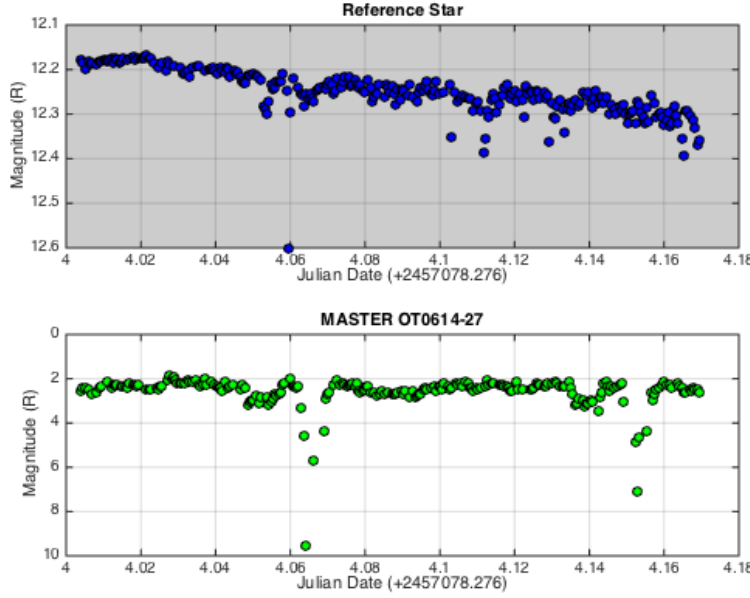


Fig. 12.— This is a light curve for MASTER OT0614-27 on the 28th of February 2015. It is obtained with the 1.0 m telescope using the R filter.

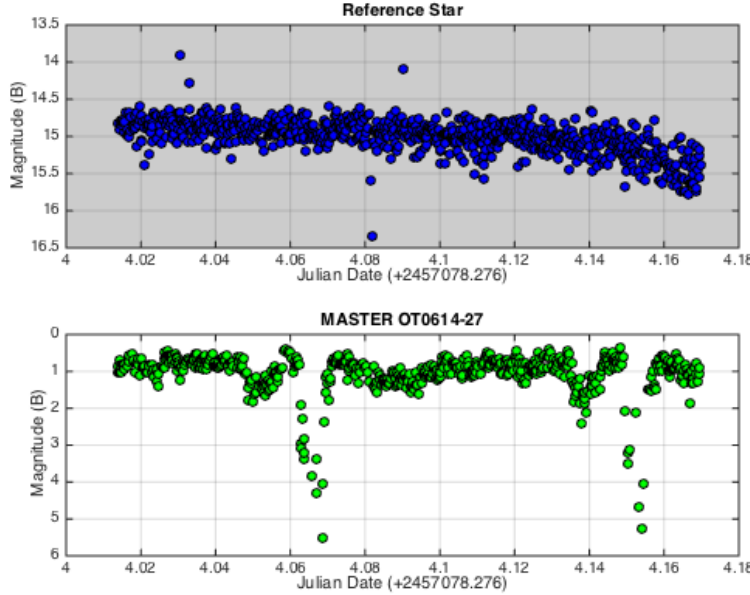


Fig. 13.— This is a light curve for MASTER OT0614-27 on the 28th of February 2015. It is obtained with the 1.9 m telescope using the B filter.